IEEE Photonics Journal
An IEEE Photonics Society Publication

Open Access

Indoor High Precision Three-Dimensional Positioning System Based on Visible Light Communication Using Particle Swarm Optimization

Volume 9, Number 6, December 2017

Ye Cai
Weipeng Guan
Yuxiang Wu
Canyu Xie
Yirong Chen
Liangtao Fang

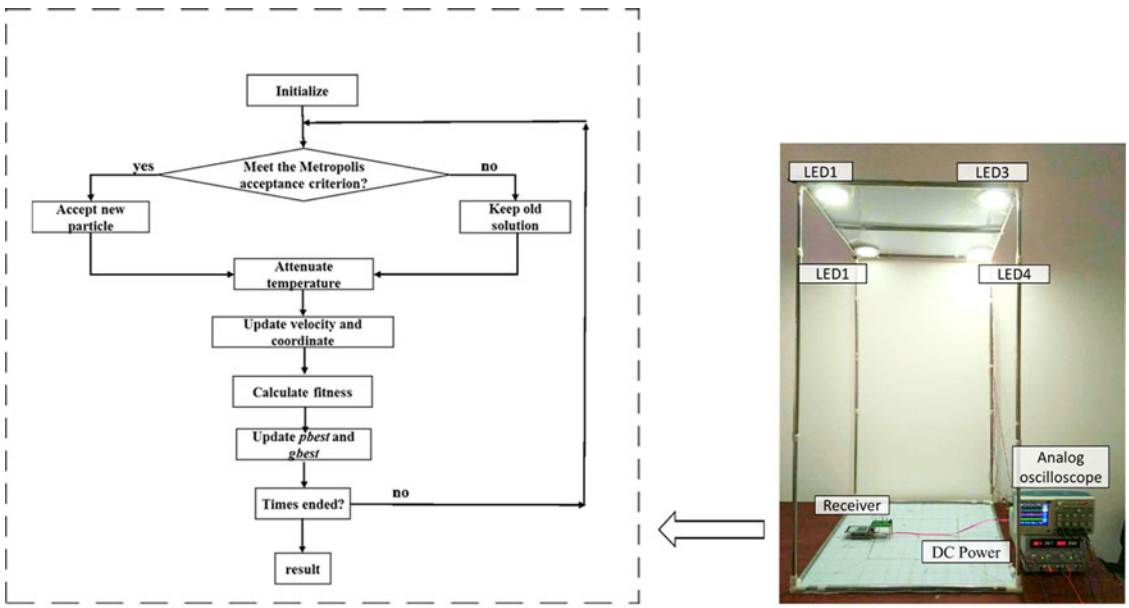

DOI: 10.1109/JPHOT.2017.2771828
1943-0655 © 2017 IEEE

Indoor High Precision Three-Dimensional Positioning System Based on Visible Light Communication Using Particle Swarm Optimization

Ye Cai,[1] Weipeng Guan,[1] Yuxiang Wu,[1] Canyu Xie,[2] Yirong Chen,[3] and Liangtao Fang [1]

[1]School of Automation Science and Engineering, South China University of Technology, Guangzhou, Guangdong 510640, China
[2]School of Materials Science and Engineering, South China University of Technology, Guangzhou, Guangdong 510640, China
[3]School of Electronic and Information Engineering, South China University of Technology, Guangzhou, Guangdong 510640, China

DOI:10.1109/JPHOT.2017.2771828

Manuscript received September 13, 2017; revised October 25, 2017; accepted November 6, 2017. Date of publication November 13, 2017; date of current version November 30, 2017. This work supported in part by the National Undergraduate Innovative and Entrepreneurial Training Program (201510561003, 201610561065, 201610561068, 201710561006, 201710561054, 201710561057, 201710561058, 201710561199, 201710561202) and in part by the Special Funds for the Cultivation of Guangdong College Students' Scientific and Technological Innovation ("Climbing Program" Special Funds) (pdjh2017b0040). Corresponding author: Weipeng Guan (email: gwpscut@163.com).

Abstract: Recently, visible light communication (VLC) has gradually become a research hotspot in indoor environments because its advantages of illumination and relative high positioning accuracy. But unfortunately, in the matter of algorithm complexity and positioning accuracy, most existing VLC-based systems fail to deliver satisfactory performance. Moreover, the majority of visible light positioning algorithm in them are based on two-dimensional (2-D) plane. In addition, some of the systems realize 3-D positioning on the base of various sensors or hybrid complex algorithm. These methods greatly reduce the robustness of VLC system. To solve these problems, a novel VLC positioning system based on modified particle swarm optimization (PSO) algorithm is put forward in this article. PSO is a powerful population-based stochastic approach to solve the global optimization problems, such as VLC-based indoor positioning, which can be transformed into a global optimization problem. Our simulation shows that the average distance error is 3.9 mm within 20 iterations in an indoor environment of 3 m $\times$ 3 m $\times$ 4 m. And the positioning results prove that this system can prove high localization accuracy and significantly lower the algorithm complexity. Moreover, in the experiment, we come up with a solution that using Kalman filter to deal with the unstable received signals. Our experiment result proves the mentioned system satisfies the requirement of cm-level indoor positioning. Therefore, this scheme may be considered as one of the competitive indoor positioning candidates in the future.

Index Terms: Visible light communication (VLC), indoor positioning systems (IPS), particle swarm optimization (PSO), positioning accuracy, simulated annealing (SA).

1. Introduction

Indoor positioning has been a topic of growing interest for the last few years as the demand for accurate location-based services (LBS). Due to the wide application scenarios such as large shopping malls and underground parking lots, the demand of high accuracy indoor positioning is larger and larger. However, traditional indoor positioning systems such as wireless local area network (WLAN), Zig bee, Ultra Wideband (UWB), Bluetooth and Radio-frequency Identification (RFID) deliver positioning accuracies from tens of centimeters to a few meters. Therefore, a high accuracy LED-based indoor positioning system using visible light communication (VLC) technology is put forward. This system can offer advantages as followed. First, communications using radio-wave approaches is more vulnerable to multipath effects than visible light, which means a higher positioning accuracy can be achieved with VLC technology; second, in some environments such as hospitals and airplanes, radio frequency (RF) radiation is hazardous or even forbidden, while VLC-based approaches can fit in perfectly since no RF interference will be generated by LEDs. Last but not least, services can be provided universally so long as lighting infrastructures exist, thus hardware cost is minimized [1]. Positioning systems based on VLC can be divided into two formats: photodiode-based (PD-based) and image sensor-based [2]. As an image sensor-based positioning system usually need to use image processing techniques which sets a great demand on system performance, the simplicity, reliability and low cost of PD-based positioning system show wide application in indoor positioning field [3]. To date, visible light positioning (VLP) based on PD has been deeply explored and there are some measurements to calculate the location of terminal such as time of arrival (TOA), time difference of arrival (TDOA), angle of arrival (AOA) or received signal strength (RSS). To take the cost, difficulty and accuracy of indoor positioning into consideration, RSS based positioning is preferred due to its low cost and high accuracy [4]. Hence, the distance from the LED to the terminal can be determined by the gain differences. At the same time, multiple LED transmitters or optical receivers are often used to achieve the gain difference for indoor localization. However, when using multiple transmitters, the inter-cell interference (ICI) may be a serious problem in VLP. Therefore, In our prior works [5]–[7], to reduce inter-cell interference caused by the presence of multiple reference points in the positioning system, the visible light from LED base stations installed on the ceiling was modulated in code division multiple access (CDMA) at different spreading code, which realizes the code division multiplexing to separate the overlapping signals in time domain and frequency domain. And the effectiveness and performance of the CDMA in VLP was well documented, so it will not be in-depth description in this paper. For the readers that are interested in the CDMA, please refer to our previous reports.

There are many previous work realizing the 3-D positioning by VLC as we mentioned. To realize the 3-D positioning, the height of the receiver must be determined. However, some of these method to estimate the height value and the two-dimensional plane value respectively. For example, in [8], Li Qing-Lin *et al.* divided the 3-D space into numerous 2-D planes. In each 2-D plane, various azimuth angles and the angle gain difference can be achieved. According to the difference of the angle gain, a 3-D positioning algorithm is proposed to realize a positioning average accuracy of 3.5 cm. And some of the methods are relatively complex. In [9], Yang Se-Hoon *et al.* used a single transmitter and multiple tilted optical receivers to realize 3D indoor positioning based on gain difference, which is a function of the AOA and the RSS. Moreover, some even have a limitation of positioning height. In [10], Gu Wenjun *et al.* presumed the height in the prediction stage, and nonlinear estimation is applied in the correction stage to realize three dimensional coordinate estimation which just varies from 0.7 m to 1.7 m considering user's hand height and vertical movement. And some estimate the position by applying other sensors or equipment. In [11], Yin Liang *et al.* use an angle diversity transmitter associated with accelerometers for uplink three-dimensional localization. In [12], Wang Yuqi *et al.* used the front camera of mobile phone and the proposed collinear equation model to realize a level of decimeter 3-D positioning error. In [13], Xu Yinfan *et al.* employ two annular receivers with multi-photodiodes installed on the ceiling to locate the terminal who carry LEDs, and the positioning error is below 0.2 m. According to what have been discussed above, some of these methods are complex for based hybrid positioning algorithm, or the positioning accuracy is not high,

or even the range of height estimation is limited, which is not a real 3-D positioning but just the small range approximation. In addition, some of these method to respectively estimate the height value and the two-dimensional plane value will greatly improve the computation time.

In this paper, we creatively come up with a 3-D positioning system based on modified particle swarm optimization (PSO) improved by simulated annealing (SA) algorithm to solve the problem above. PSO is a powerful population-based stochastic approach to solve the global optimization problems [14], such as VLP, which can be transformed into a global optimization problem [15]. By simulating the group behavior of animals, both the particle swarm and the individual particle are able to evolve, then the optimal solution is obtained to calculate the 3-D coordinates of the terminal [16]. In the meanwhile, to deal with the problem of premature convergence in PSO and improve the speed of finding the optimum object, SA-PSO is put forward. SA algorithm is based on the analogy between the simulation on the annealing of solids and the problem of solving combinatorial optimization problem [17]. Therefore, the proposed system based on VLC technology can be used to determine the coordinate of the terminal by the algorithm mentioned above. And our simulation shows that this system performs very well. As for experiment, in real situation, owing to background noise, NLOS propagation and other uncertain signal interference, the received signals are very unstable, which cause great positioning error if we receive the signal for only once to locate a position. And as we know there are few consideration about this problem in the existing reports. Therefore, we come up with a solution that using Kalman filter to filter the received signal. Kalman filter predicts the next state of the object based on its prior assumptions and corrects its prediction using the incoming measurement of the state. This prediction is used as the initial state for the next time step. And this process repeats recursively [18]. Moreover, owing to the actual channel gain does not follow the ideal channel model [19], we also make some adjustment for the parameters in the channel model to improve the positioning accuracy.

The contribution of our work can be detailedly listed as followed. First we proposed a novel 3-D positioning system based on modified PSO to greatly improve the position accuracy and decrease the computation time. Second, our system reflects the real situation more and supports user's mobility. According to our simulation, even when the receiver is moving at a speed of 1 m/s, the average position accuracy is still very high. Third, unlike other existing VLP system, we filter the received signal by using Kalman filter, which improves the VLP accuracy greatly in real situation. The remainder of the paper is organized as follows. Section 2 details the system model of the VLP system, and provides details of the proposed PSO algorithm. Section 3 and Section 4 describes the simulations results and experiment results respectively to verify the proposed approach. Then we conclude our paper in Section 5.

2. System Principle and Positioning Algorithm

2.1 System Model

As shown in Fig. 1, the proposed VLP system is applied in an indoor environment and all LEDs are installed on the ceiling to satisfy the requirement of lighting. The coordinates of them can be labeled as (X_j, Y_j, Z_j), (j = 1, 2, 3, 4), respectively. Each of LEDs is assigned a unique signal which represents the coordinate of itself. The signals are transmitted from LEDs to the receiver that is placed on the floor by visible light communication (VLC) technique. Here, the radiant intensity of a LED can be assumed to follow a Lambertian radiation pattern due to its large beam divergence. The line-of-sight (LOS) channel gain $H(0)$ can be given by [20] if we assume $\theta = 0$:

$$H(0) = \begin{cases} \frac{(m+1)A}{2\pi d^2}\cos^m(\phi)\cos(\psi)T_s(\psi)G(\psi), & 0 \le \psi \le \psi_C \\ 0, & \psi \ge \psi_C \end{cases} \quad (1)$$

where the parameters are as follows. m is the Lambertian order and defined as:$m = \frac{-ln2}{\ln(\cos(\phi_{1/2}))}$, where $\phi_{1/2}$ is the semi-angle at half illuminance of a LED. A is the area of an optical detector.d is the distance between LED anchor nodes and the positioning terminal. $T_s(\psi)$ is the gain of an optical filter, and $G(\psi)$ is the gain of an optical concentrator given by G $(\psi) = \frac{n^2}{sin^2(\psi_c)}$,with n denoting

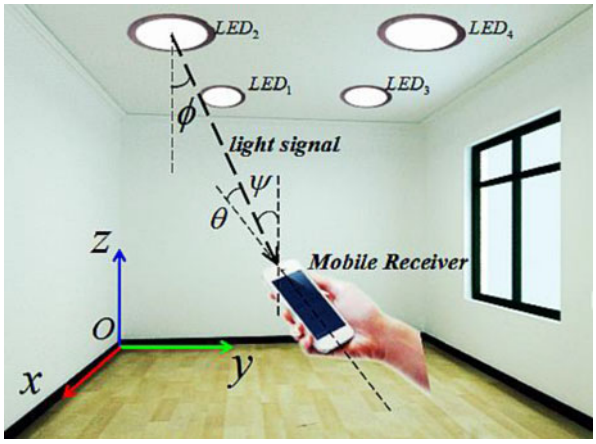

Fig. 1. The scene graphic of indoor positioning based on VLC.

the refractive index of the optical concentrator. ϕ is the irradiant angle, ψ is the incident angle, and ψ_C is the field-of-view of the receiver. When the emitted optical power P_t is received by the receiver, the incident optical power from LOS path P_{LOS} can be given by $P_{LOS} = P_t \times H(0)$, and the corresponding electrical power P_r is given by $P_r = R\lambda P_{LOS}$, where R is the equivalent impedance of the receiver, and λ is the responsivity of the optical detector. In VLP system, there are no optical filter and concentrator, and therefore, we can get

$$P_r = \frac{C}{d_j^2} \cos^m(\phi)\cos(\psi) \tag{2}$$

Where C is a constant and defined as

$$C = \frac{R\lambda A\,(m+1)\,P_t}{2\pi} \tag{3}$$

C, m are constants related to the VLP system. To relax the complex conditions, if we suppose that the two-dimensional space of the terminal is parallel to the ceiling plane, so incidence angle and radiation angle are the same. $\phi = \psi = \cos^{-1}\frac{H-h}{d_i}$, H is the total height of the positioning unit, and h is the height of the positioning terminal plane.

In practical system, the total incident optical power P_r of the terminal contains the ambient light power P_{bg}, the incident optical power P_{LOS} from LOS path and NLOS path P_{NLOS}. In general, only P_{LOS} is used for positioning in LPS, while P_{NLOS} and P_{bg} are both viewed as noise power [21] [22]. In this paper, we primarily employ thermal and shot noise components with normal distribution, and the total noise variance can be given as

$$N = \sigma_{shot}^2 + \sigma_{thermal}^2 + R(\lambda\, P_{NLOS})^2 \tag{4}$$

where σ_{shot}^2 is the shot noise variance which is depended on the total incident optical power, and $\sigma_{thermal}^2$ is the thermal noise variance which is depended on the receiver's parameters. σ_{shot}^2, $\sigma_{thermal}^2$ and P_{NLOS} are all described detailedly in [23]. The signal-to-noise (SNR) due to LOS path can be defined as

$$SNR = 10\log_{10}\left(\frac{P_r}{N}\right) \tag{5}$$

2.2 Modified Particle Swarm Optimization Designed for VLP

Considering that the precision of existing VLP methods is not very high, we proposed a creative positioning system based on SA-PSO, which is a powerful population-based stochastic approach

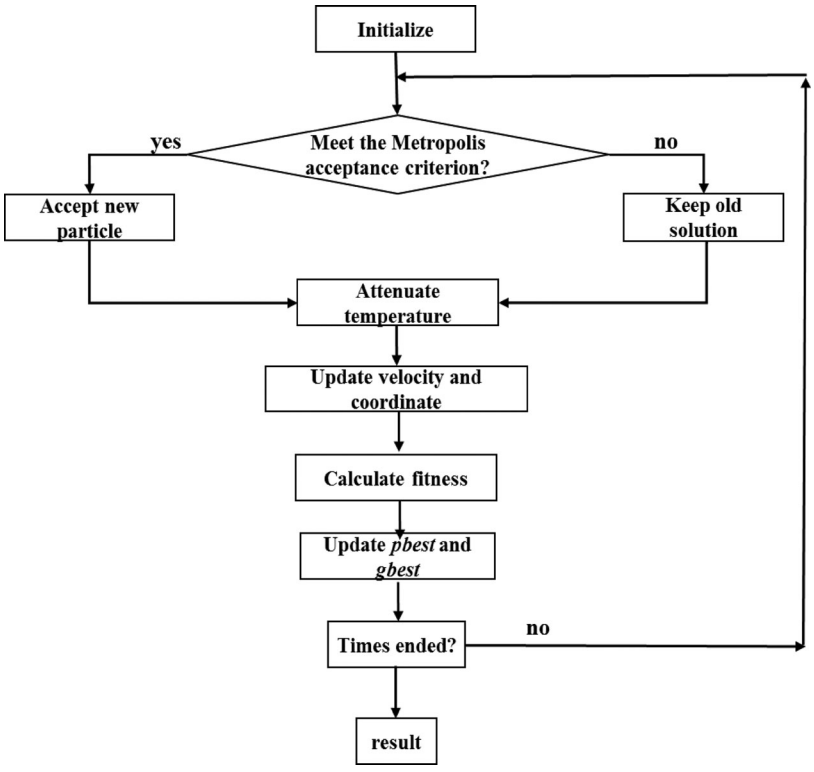

Fig. 2. Modified PSO algorithm flow diagram.

to solve the nonlinear global optimization problems. According to the system model above, the VLC positioning problem can be transformed into a global optimization problem and position of the terminal can be calculated by solving the (1), where the channel gain $H(0)$ has been calculated by the received power. We proposed a creative positioning system based on PSO to locate the terminal position. The mentioned positioning algorithm includes three steps: (1) Setting initial value; (2) Update particles according to simulated annealing; (3) Particle swarm optimization iteration. The details of the algorithm is given in Fig. 2, which is told as followed:

Step 1. **Setting initial VLP value**

The first iteration particles of PSO algorithm are randomly set in the room. So, firstly, set the particle group size N, the max iteration number $m_{\max}$. Give each particle a random coordinate (X, Y, Z) as an initial position of the terminal in VLP system and a random velocity (v_x, v_y, v_z). The position is surely limited by the room's size. Then, calculate the fitness of every particle using the fitness function given below. According to the model given above, the fitness function can be expressed as follow if we assume m as 1:

$$d_j = \sqrt{(X - X_j)^2 + (Y - Y_j)^2 + (Z - Z_j)^2} \tag{6}$$

$$H(0)'_j = \frac{(m+1)A}{2\pi d^2} \cos^m(\phi) \cos(\psi) T_s(\psi) G(\psi) = \frac{C(H-h)^2}{{d_j}^4} \tag{7}$$

$$Fitness_j = \sum_{j=1}^{4} \left(H(0)'_j - H(0)_j\right)^2 \tag{8}$$

Where d_j is the physical distances between a particle and four LEDs ($j = 1, 2, 3, 4$), respectively. Here, $H(0)_j$ represents the channel gain between every LED and the terminal. So, fitness of each particle to each LED: $Fitness_j$ can be calculated by (6)–(8), which means that coordinates of the particle with very small fitness can be regard as the estimated position. Therefore, we

search the particle with minimum fitness as the best position in the whole group named "*gbest*", and set the original position of a particle as its best position in its history named "*pbest*". In the meanwhile, we use SA to deal with the problem of premature convergence in PSO and improve the speed of finding the optimum object. The initial temperature T_0 in SA algorithm can be determined by:

$$T_0 = -\frac{f_{gbest}}{\lg 0.2} \tag{9}$$

where f_{gbest} is the fitness of *gbest* in first iteration. Next, repeat steps 2 and 3 iteratively until the iteration number reaches the max iteration number *m*.

Step 2. **Update Particles According to Simulated Annealing**

The Metropolis acceptance criterion of SA can be given by:

$$P_i = e^{-\frac{f_i - f_{gbest}}{T_n}} \tag{10}$$

Where f_i ($i = 1, 2, 3,..N$) is the fitness of *i*th particle, T_n is given by:

$$T_n = \lambda T_{n-1} \tag{11}$$

where λ is the attenuation parameter and *n* means the iteration time. If $P_i. > c$, then accept P_i as the new *gbest* in the group. C is a random number between 0 and 1.

Step 3. **Particle Swarm Optimization Iteration**

1) Update every particle's velocity and coordinate in each direction

The iteration process follows these two equations:

$$\begin{cases} X_{n+1} = X_n + v_x \\ Y_{n+1} = Y_n + v_y \\ Z_{n+1} = Z_n + v_z \end{cases} \tag{12}$$

Where *n* means the times of iteration.

$$v_{n+1} = \omega \cdot v_n + r_1 \cdot c_1 \times (pbest_n - p_n) + r_2 \cdot c_2 \times (gbest_n - p_n) \tag{13}$$

where v_n is the velocity of a particle in its *nth* iteration, p_n is the particle position in the *nth* iteration, c_1 and c_2 are two acceleration coefficients, and $pbest_n$ and $gbest_n$ are personal best position and global best position in the *nth* iteration. r_1 and r_2 are two random constriction coefficients in the range (0, 1) sampled from a uniform distribution. The implementation of constriction coefficients can prevent explosion and induce particles to converge on optima. ω is the inertia factor which control the convergence of particles. In this step, we update the velocity and the coordinate of each particle according to (13) and (12) respectively. Moreover, we also make some improvement for the algorithm: If the coordinate of the particle is out of the room, then move this particle randomly to the neighborhood of *gbeat.*

1) Update fitness, "*pbest*" and "*gbest*"

After updating velocity and coordinates, every particle's fitness need to be updated according to the fitness function (6)–(8) in Step 1. In each iteration, every particle keeps tracking "*pbest*" and "*gbest*" to move toward the optimal solutions. We update *gbest* and change the "*pbest*" if a particle's new fitness is smaller than its old one.

3. Simulation and Analysis

3.1 Three-Dimensional Positioning Simulation Model

Simulation is launched to evaluate the performance of our mentioned algorithm. In this section, an indoor visible light positioning system with a 3 m × 3 m × 4 m environment is established as shown in Fig. 1. Each LED transmits a unique signal and receive by the positioning terminal. The main parameters of the model can be seen in Table 1;

TABLE 1
Simulation Parameters

Parameter	Reference
Indoor space unit size (L × W × H) /m	3 m × 3 m × 4 m
Position of the four LED s (x, y, z) /m	LED1 (0, 0, 4) LED2 (3, 0, 4) LED3 (3, 3, 4) LED 4 (0, 3, 4)
Height of the receiver /m	0.5 to 3.3 (resolution:0.7)
Plane range of the receiver /m	(0.5, 0.5) to (2.5, 2.5) (resolution:0.2)
Test position	(1.5, 2.0, 0.5)
Transmitter power /W	10
The FOV of the transmitters /deg	60
The FOV of the receiver /deg	120
The effective area of PD /cm^2	1.0
The photoelectric transformation efficiency /A · W^{-1}	0.35
The gain of optical filter [$T_s(\phi)$]	1.0
The gain of optical concentrator [$G(\phi)$]	1.0
Particle group size	200
Max iteration times	20
attenuation parameter	0.5

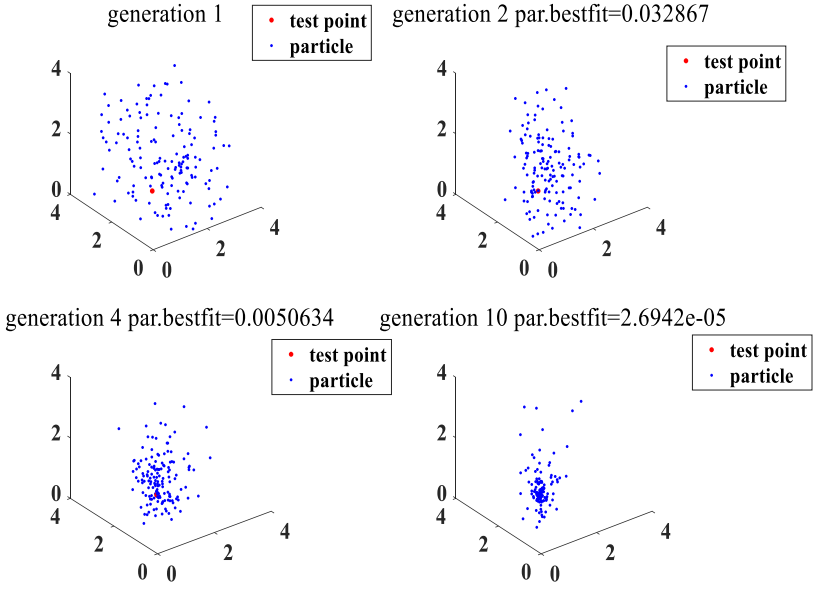

Fig. 3. Convergence progress of the modified particle swarm optimization algorithm.

3.2 Results and Analysis

3.2.1 Iteration Times Analysis: Fig. 3 shows the convergence process of the mentioned algorithm. In this figure, red dot whose coordinate is (1.5, 2.0, 0.5) is a test point, and the blue dots represent the particle swarm. As we can see, the first generation particles are set randomly in the

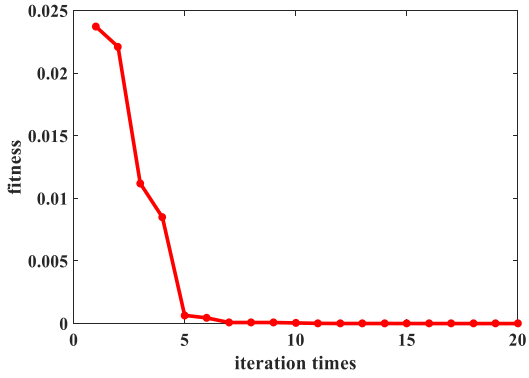

Fig. 4. The relationship between iteration times and the best fitness of the particle swarm.

room, and they move toward the optimum solution rapidly generation by generation. After 10 generations, most of the particles are gathering in the neighborhood of the test point and the minimum fitness of the particle swarm is 2.6942×10^{-5}, while the coordinate of this particle is (1.4976565, 1.9996543, 0.5017855). The position error is 2.96 mm. In the meanwhile, if the iteration time is set to 20, the coordinate of the optimum particle is (1.4999874, 2.0002786, 0.5000784), and the error is close to 0. So if the former error can be accepted, the position can be located at the 10th evolutionary generations. Fig. 4 shows the relationship between fitness of the optimum particle and the iteration times, which proves that our algorithm can serve high accuracy and good speedability by comparing with other algorithm. For example, in [24], the author use traversal search to locate the receiver. Though he was focusing on the positioning accuracy, it can't be avoided that traversal search is much more complex than PSO. For instance, if we want to reach an mm-level accuracy in this simulation, traversal search needs $3000 \times 3000 \times 4000$ iterations with a step of 0.1 cm, and algorithm mentioned only need 20 iterations. Therefore, under the same hardware condition, our algorithm has less complexity and undoubtedly superior to many other algorithm.

3.2.2 Multi-Point Testing: The whole simulation result of 3-D dimension positioning is discussed in this section. The resolution of the test positions is 0.7 m from 0.5 m to 3.3 m in the room and 605 positions are included. All of them are respectively shown in Fig. 5 for readers, where the symbol "x" represent the estimated position and the circles represent the real position. We can tell from Fig. 5 that the proposed positioning system performs very well in the whole room.

As the Fig. 6 shows, the positioning algorithm performs well in this situation, and most of the error is under 1 cm. The average of them is 3.9 mm. If 90% of the test points are considered accepted, the 3-D position error CDF curve in Fig. 6 shows that the test points have a maximum error of 7.159 mm. In order to better present the error, the distribution of 90% of the errors is presented in Fig. 7. We can tell from it that most of the positioning error are within 2 mm, which proves the algorithm perform very well.

3.3 Extended Simulation and Result Analysis

3.3.1 Positioning in Motion Scene: In our simulation, a random path is given by assuming a moving target in the room at a speed of around 1m/s, and there are 251 samples in total.

Fig. 8 shows that the algorithm performs well in motion scene. In this figure, the blue line is the path and the red spots are the estimated positions that track the path. In order to better present the result, Fig. 9 shows the horizontal view and the vertical view of the positioning results. The results shows that with the proposed algorithm, the estimated results follow the path very well as we can see. To present the 3- D positioning result directly, Fig. 10 shows the histograms of positioning errors of this system. It shows the histogram of 3-D, horizontal and vertical positioning errors, respectively. As we can see, over 90% of the position errors are within 0.5 cm, which proves that the algorithm above performs very well in motion positioning scene.

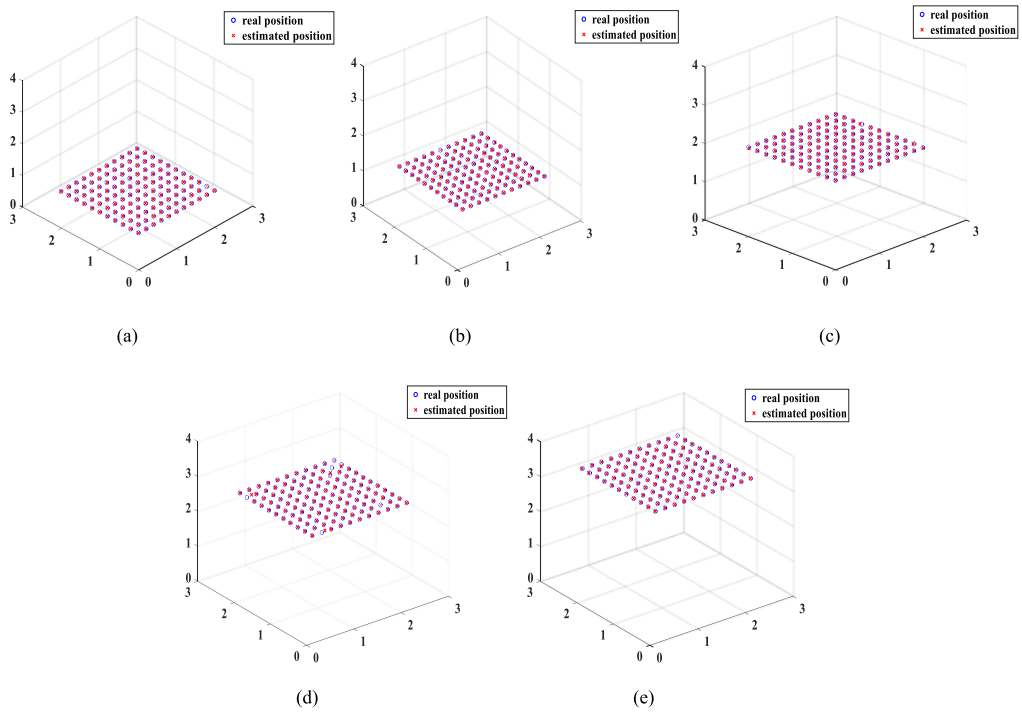

Fig. 5. The distribution of the real position and its estimated 3-D position. (a)–(e) represent the 3-D positioning results at the height of 0.5 m, 1.2 m, 1.9 m, 2.6 m, 3.3 m, respectively.

3.3.2 Other Extended Simulation: In the former simulations, the receiver is set horizontally which is adopted in most papers about indoor positioning system based on VLC. But in the real application situation, a receiver may not lay horizontally such as in Fig. 11. It means that the irradiant angle will changes while the incident angle stays. Therefore, the formula (1) is needed to change if we take the angle of the reciever into consideration, or it will cause position error. So, the formular can be express as:

$$H = \frac{(m+1)A}{2\pi d^2}\cos^m(\phi)\cos(\psi)T_s(\psi)G(\psi) = \frac{C(H-h)}{d^3}\cos^m\left(\cos^{-1}\left(\frac{H-h}{d}\right)+\theta\right) \tag{14}$$

And the new fitness can be calculated by:

$$d_j = \sqrt{(X-X_j)^2+(Y-Y_j)^2+(Z-Z_j)^2} \tag{15}$$

$$H'_j = \frac{C(H-h)}{{d_j}^3}\cos^m\left(\cos^{-1}\left(\frac{H-h}{d_j}\right)+\theta\right) \tag{16}$$

$$Fitness_j = \sum_{j=1}^{4}\left(H(0)'_j - H(0)_j\right)^2 \tag{17}$$

So we conduct our simulation by the new fitness function above and the result and analysis are as followed:

In order to better present the result, angle θ which is between the normal of receiver and the vertical direction, is set as from 0 deg to 20 deg (resolution is 5 deg), such as in Fig. 11. And each of the tilt angles has 121 positions tested at the height of 1.5 m. Fig. 12 shows the 3-D positioning result. It implies the mentioned system performs very well when the angle is small. Furthermore, as we can see, owing to the tilt angle, the positioning error decrease because the fitness function

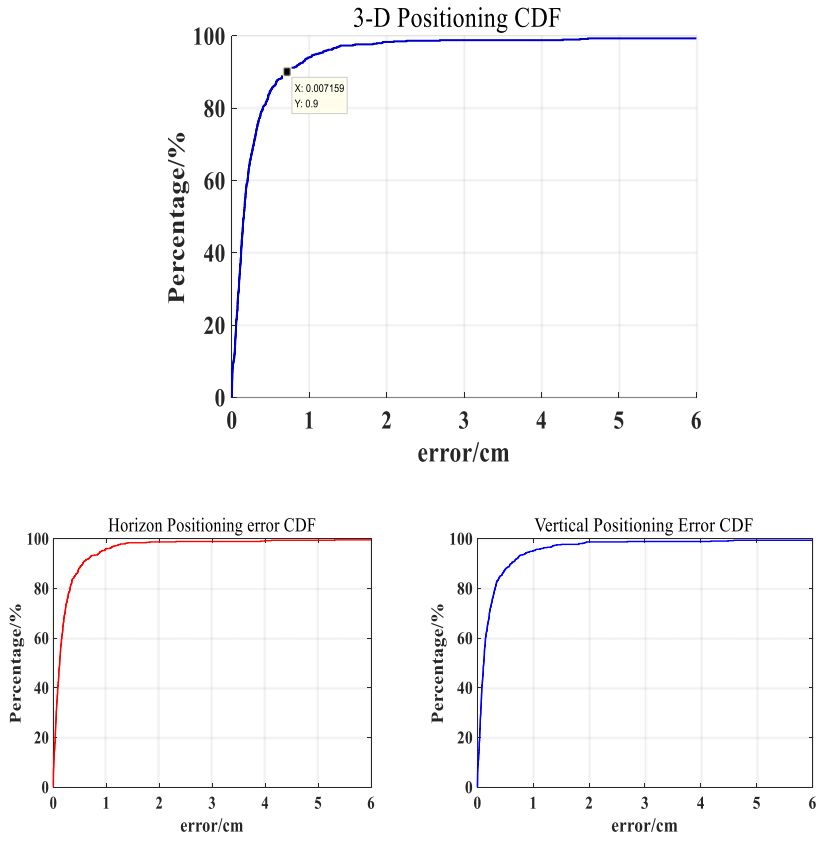

Fig. 6. The cumulative distribution function (CDF) curves of positioning error.

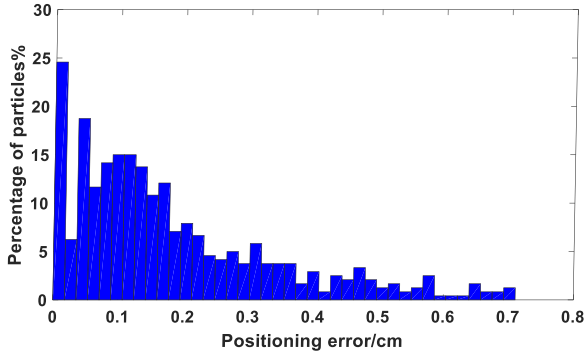

Fig. 7. Histogram of 90% of the positioning error.

changes. Comparing with the old function (6)–(8), the new fitness function (15)–(17) has added a new parameter θ, which increase the complexity of the calculation but improve the positioning accuracy. However, the accuracy deteriorates when the angle is set too steep because the light intensity received by receiver is decrease or even reduce to 0. Moreover, the error also increase if the height is set so high that leads to the received power decrease. For example, in Fig. 13, the positioning error increase with the height when the tilt angle is set to 20 deg.

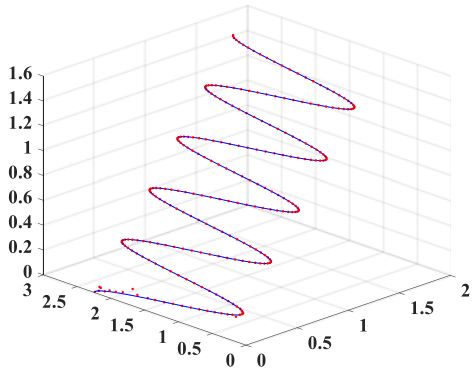

Fig. 8. Three dimention positioning result in motion scene.

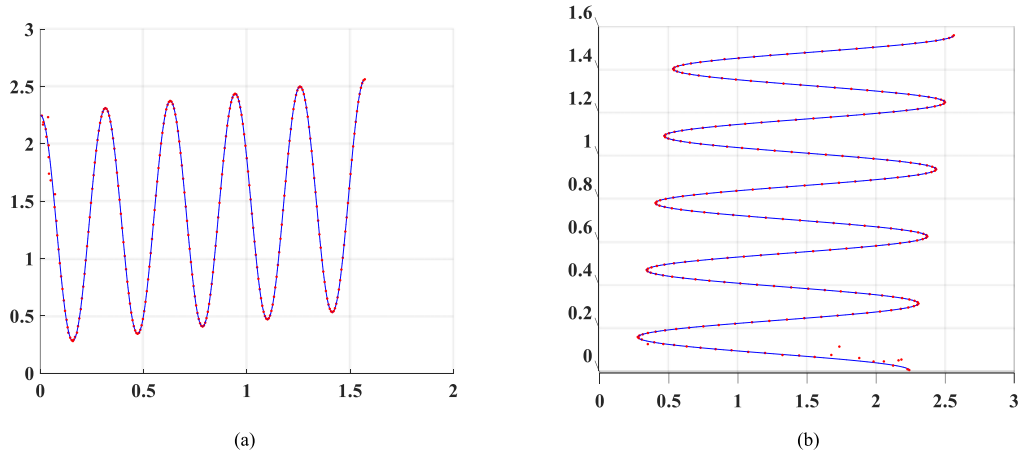

Fig. 9. The horizontal view and vertical view of positioning result respectively. (a) Horizontal view. (b) Vertical view.

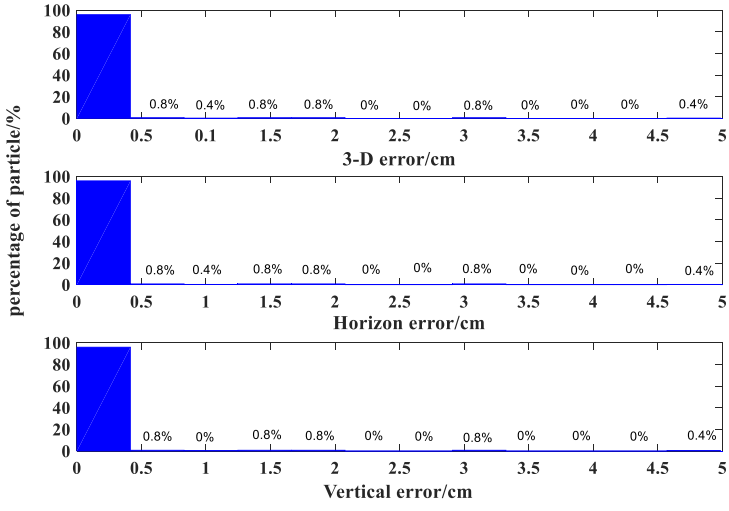

Fig. 10. Histogram of positioning error in motion scene.

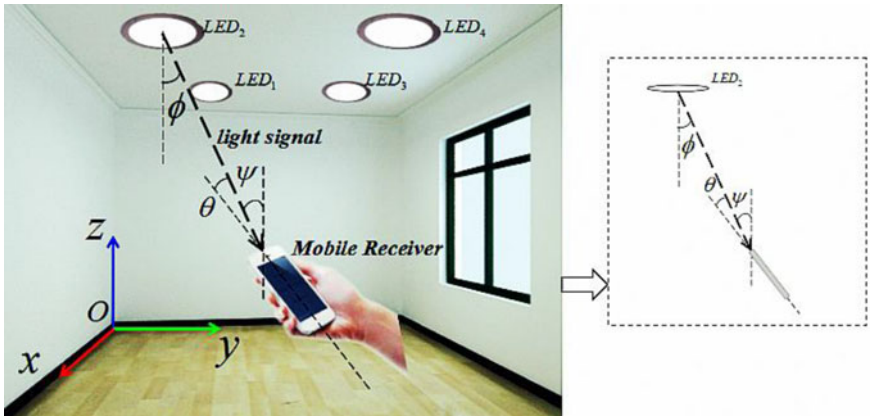

Fig. 11. VLP system whose receiver has a tilt angle in real situation.

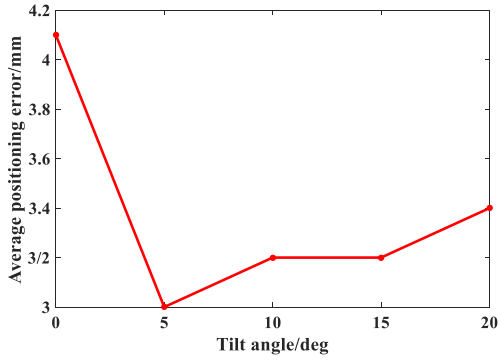

Fig. 12. Location error varies with the tilt angle θ.

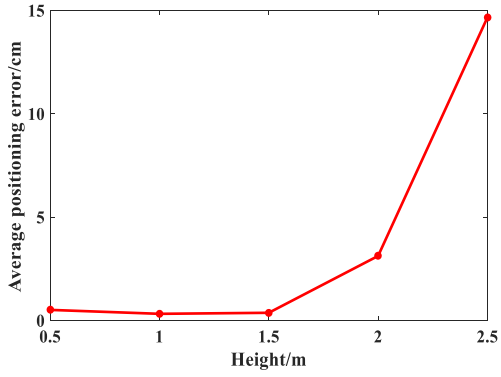

Fig. 13. Location error varies with the height.

4 Experiment Setup and Result

4.1 Experiment Setup

Hardware design: The experiment is established to verify the feasibility of the system and validate our theoretical analysis shown in Fig. 14. Four LEDs as signal generator are installed in a cube frame with a size of 0.9 m $\times$ 0.9 m $\times$ 1.5 m^3. They are white (6000 K) LED downlights (KECENT, KC-CBF09). Each of them has 45 white phosphorescent SMD LEDS (Everlight, 2835, 0.2 W),

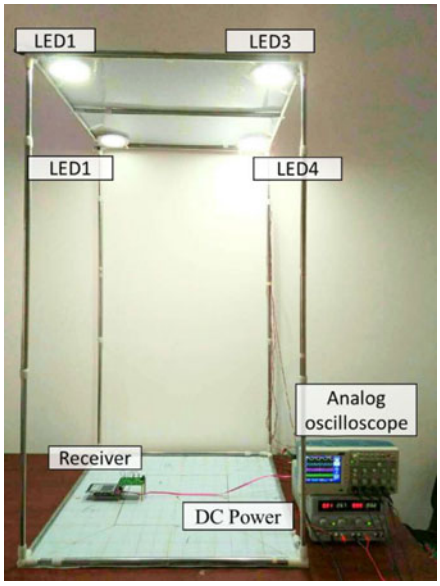

Fig. 14. Experimental platform of VLC system based on modified PSO.

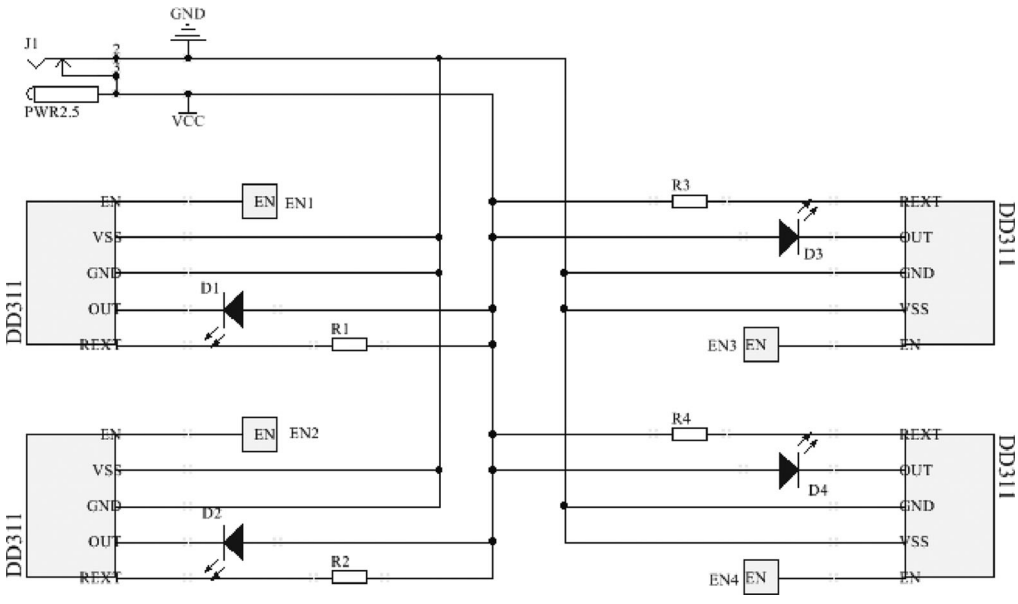

Fig. 15. The circuit diagrams of transmitting terminal.

driven in series, which are arranged in an annular pattern inside the downlight. We intend to provide positioning and lighting simultaneously. Current drive circuit (DD311) apply the resulting waveform to the LEDs and the PIN diode (S6968) detect the light signals, whose frequencies are set 400 Hz, 800 Hz, 1600 Hz and 3200 Hz respectively. And the signals can be seen in the analog oscilloscope. Then they are transmitted to a stage amplifier circuit (made up of OPA657) as well as filter circuit. Then the sync signals are delivered to MCU (STM32F407ZGT6 with a 12-bit AD convertor integrated in it), where we use PSO to calculate the receiver's position. LCD attached to the receiver can display the result of positioning with the parameters (coordinates). The circuit

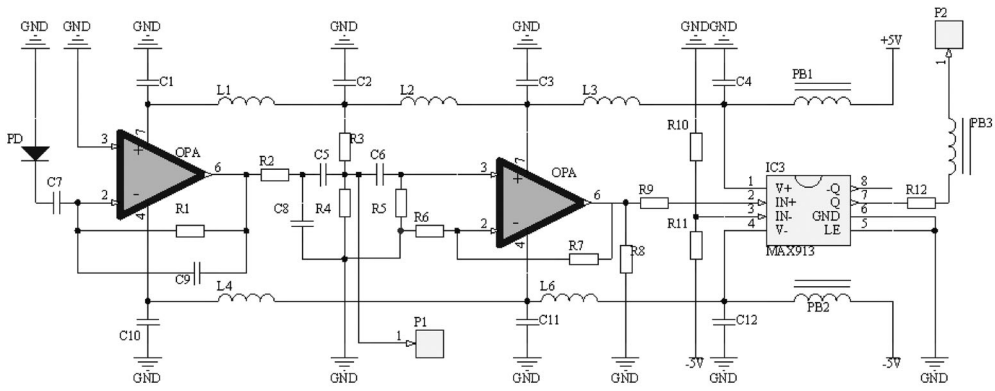

Fig. 16. The circuit diagrams of receiver terminal.

Fig. 17. The circuit board of transmitting terminal.

diagrams and circuit boards of transmitting terminal and receiving terminal are shown in Figs. 15 -18 respectively.

Signal filter: Theoretically, in one location, the received power shouldn't change over time when the transmitting signals remain unchanged. But as described above, in practical situation, background noise, NLOS propagation and other uncertain signal interference will make the received signals uncertain and influence the positioning accuracy. So, the error will be enlarged if we detect the signal for only once and locate the position immediately. In general, all of the noise above can be seen as Gaussian white noise and we use Kalman filter to deal with the received signal after the signal transmitted to MCU. Kalman filter is designed to work in a noisy environment. It can run very fast and get the optimal solution by iteration. The progress of Kalman filter can be expressed as the equation as followed:

$$\begin{cases} RSS\ (k|k-1) = A \times RSS(k-1|k-1) + BU\ (k) \\ P\ (k|k-1) = A \times P\ (k-1|k-1)\ A^T + Q \\ RSS\ (k|k) = RSS(k|k-1) + Kg\ (k) \times (Z\ (k) - N \times RSS(k|k-1)) \\ Kg\ (k) = \frac{P(k|k-1) \times H^T}{N \times P(k|k-1) H^T + R} \\ P\ (k|k) = (I - Kg\ (k)\ N) \times P(k|k-1) \end{cases} \tag{18}$$

where $RSS(k|k-1)$ is the estimated received signal strength in last state, and $RSS(k-1|k-1)$ is the optimal received signal strength in last state. $P(k|k-1)$, $P(k-1|k-1)$ are their covariance

Algorithm Kalman filter designed for RSS
Function Kalman_filter
RSS(0|0) $\leftarrow$ receive a value as the initial optimal received signal
P(0|0) $\leftarrow$ set an initial covariance
T $\leftarrow$ the recursion times in Kalman filter
k $\leftarrow$ the current state
Q $\leftarrow$ process noise covariance
R $\leftarrow$ measured noise covariance
For k = 1: T
RSS(k|k − 1) $\leftarrow$ estimated received signal in last state = RSS(k-1|k-1)
P(k|k − 1) $\leftarrow$ $P(k-1|k-1)+Q$
Kg(k) $\leftarrow$ $P(k|k-1)/(P(k|k-1)+R)$
Z(k) $\leftarrow$ the received signal in kth state
RSS(k|k) $\leftarrow$ $RSS(k|k-1)+Kg(k\times Z(k)-RSS(k|k-1)$
P(k|k) $\leftarrow$ $(1-Kg(k))\times P(k|k-1)$
Return the optimal received signal strength

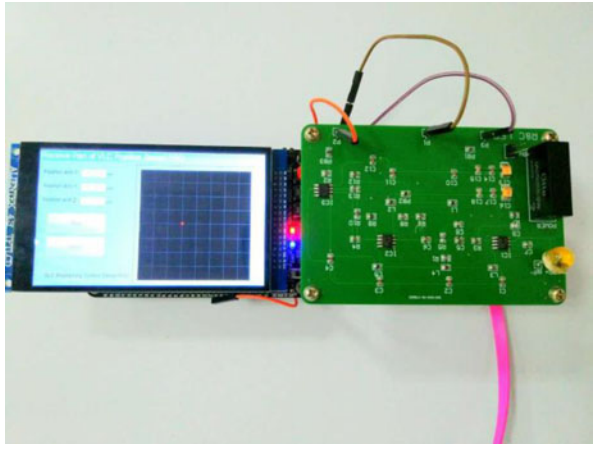

Fig. 18. The circuit board of receiver terminal and LCD attaches to it.

respectively. A, B, N are the systems parameters, Kg is the Kalman gain, $Z(k)$ is the received signal strength in kth state, I is a unit matrix, Q is the noise covariance of the process and R is the measured noise covariance. Therefore, we can use the equations above to obtain the optimal received signal and its covariance in this state. In one position, we assume A = 1, U (k)=0, N=1, I = 1. Therefore, the optimal received signal strength can be obtain by the continuous recursion. The pseudo code of Kalman filter is given in Algorithm Kalman filter designed for RSS, which can return an optical received signal.

Before conducting the experiment, we make some adjustment to the parameters of channel model, which means introduce some modification values. Firstly, we detect the received power in certain positions by applying Kalman filter, and calculate the parameters of channel model, i.e., (1) as well as the parameters of the circuits. For example, we measure the enlargement factor of the amplifier circuit for experiment to make the parameters closer to the reality. Then, we conducting our experiment on the based the model we adjusted, which can decrease the experiment error caused by theoretical channel model and designed circuits. Parameters of the experiment are shown in Table 2.

TABLE 2
Experiment Parameters

Parameter	Reference
Indoor space unit size (L × W × H) /m	0.9 m × 0.9 m × 1.5 m
Position of the four LED s (x, y, z) /m	LED1 (0, 0, 1.5) LED2 (0.9, 0, 1.5) LED3 (0.9, 0.9, 1.5) LED 4 (0, 0.9, 1.5)
Height of the receiver /m	0.4, 0.8, 1.2
Plane range of the receiver /m	(0.2, 0.2) to (0.8, 0.8) (resolution:0.2)
The effective area of PD /cm^2	1.0
Frequency of the light signals/Hz	400, 800, 1600, 3200

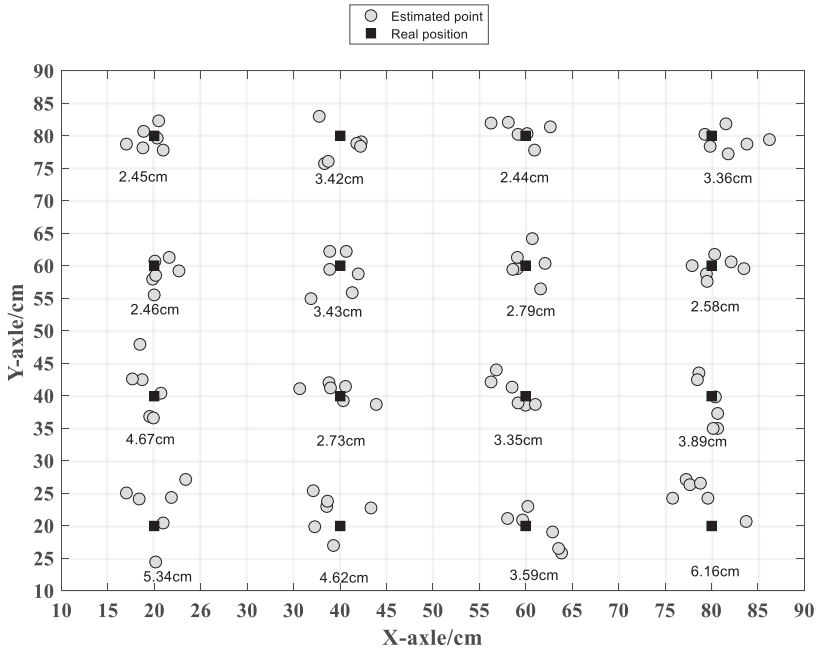

Fig. 19. Estimated position and 3-D positioning error of the experiment with the height of 0.4 m.

4.2 Result and Analyze

In the experiment, there are 16 evenly distributed test points at the height of 0.4 m, 0.8 m and 1.2 m respectively. So, 48 positions are tested in the experiment totally. Then, we locate the estimated positions by using the system we mentioned in Section 4-1. Each position is tested for 6 times and the 3-D positioning error for each location is calculated by comparing the actual spatial position and the estimated position. The position results are shown in Figs. 19-21 and the 3-D positioning average errors of the test positions are written in the figures severally

As we can see. At each test position, the proposed modified PSO algorithm is applied to calculate the position in the experiment. Experiment results suggest that the average 3-D error is 3.492 cm and the maximum error is 6.16 cm. In the meanwhile, over 80% of the errors are within 4 cm. The histograms of 3-D error, horizontal error and vertical error in each height are shown in Figs. 22-24.

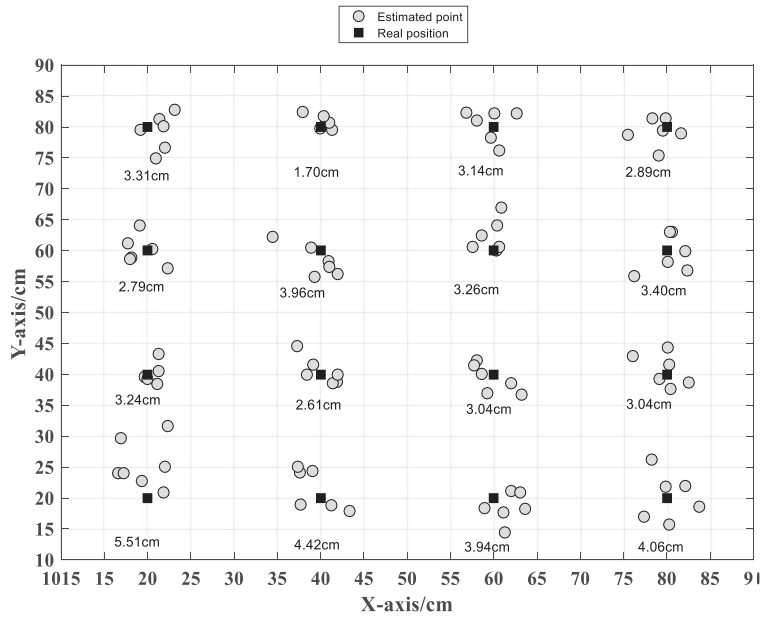

Fig. 20. Estimated position and 3-D positioning error of the experiment with the height of 0.8 m.

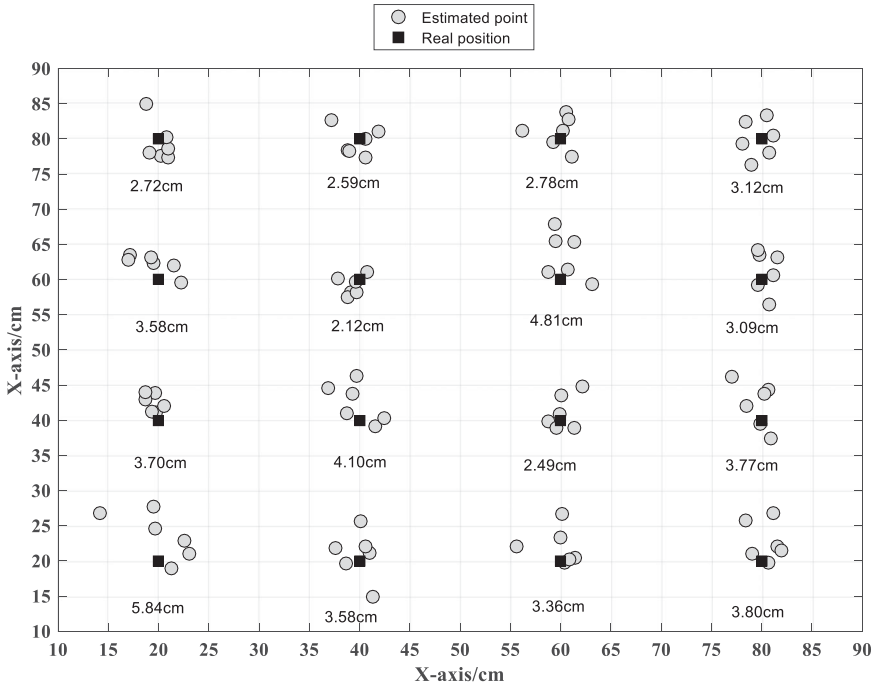

Fig. 21. Estimated position and 3-D positioning error of the experiment with the height of 1.2 m.

The results indicate that our mentioned system performs well, which is on the base of Kalman filter and modified PSO. The error is occurred by the following reasons. Firstly, some of the error is caused by the noise. Though we have adopted Kalman filter to improve the positioning accuracy, error caused by noise still can't be totally avoided. Secondly, measurement error is another factor of causing the error. For example, there are some coordinate deviation of the receiver between

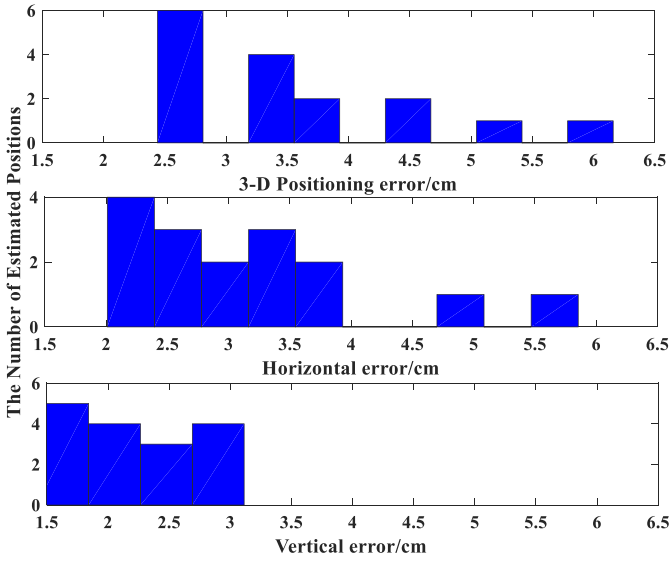

Fig. 22. Histogram of positioning error at a height of 0.4 m.

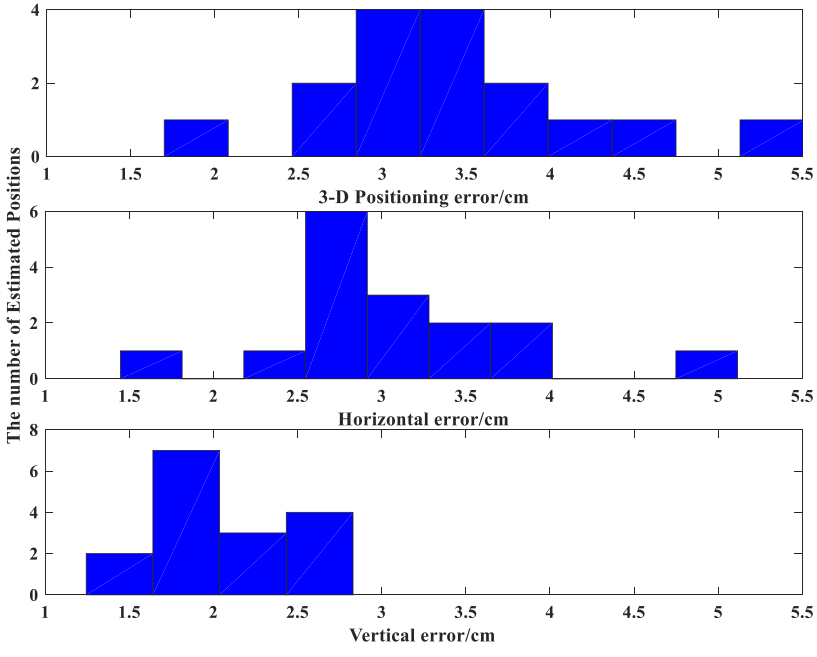

Fig. 23. Histogram of positioning error at a height of 0.8 m.

the reality and the ideal location. Finally, additional error occurred by calculation and equipment. But it is proved that the system satisfies the requirement of cm-level indoor positioning. In addition, comparing with the known VLC positioning system that we mentioned in Section 1, this system has higher precision and lower complexity.

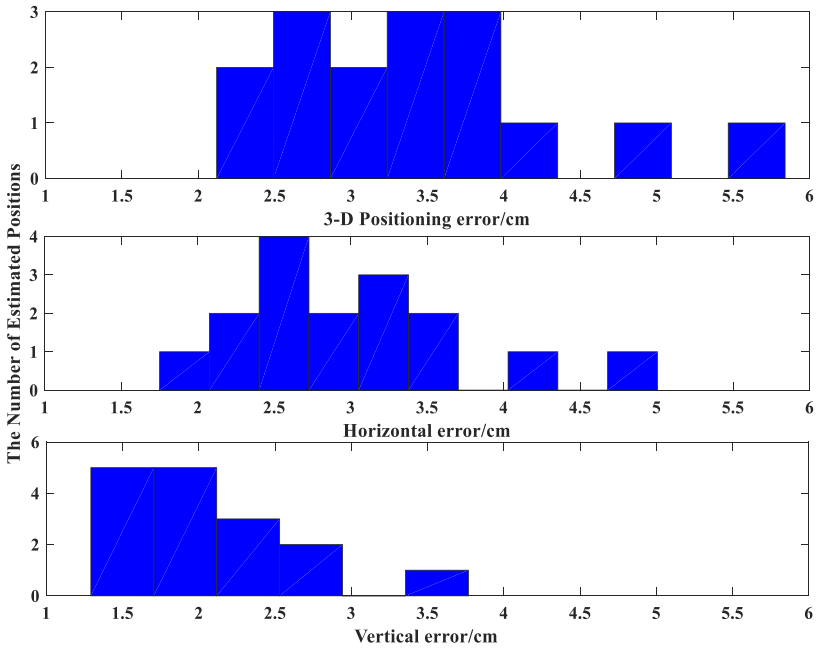

Fig. 24. Histogram of positioning error at a height of 1.3 m.

5 Conclusion

In this paper, we proposed a novel VLC-based positioning system based on modified PSO algorithm improved by SA. We transform the VLC positioning problem into a global optimization problem and use the aforementioned algorithm to solve it, for the reason that PSO is a powerful population-based stochastic approach to solve the global optimization problems. In this system, each LED transmits a unique signal to the terminal and the algorithm estimates the position according to the messages received by the terminal. By simulation, we prove that the positioning system has a high precision and good speedability, which reflects as the lower complexity of our algorithm. Our simulation result shows that the average error is about 3.9 mm. Moreover, we also do some extend simulations, which prove the mentioned system also performs well when the terminal is in a motion scene or with a small tilt angel. At last, in our experiment, in order to suppress interference signal, we propose to use Kalman filter to deal with the received signals. It is because that in practical situation, interference signals such as background noise will decrease the accuracy. And as we know there are few consideration about this problem in the existing reports. Our experiment verify that our mentioned system can achieve cm-level indoor positioning. Thus, the proposed positioning method can be used as a high accuracy and high stability in

We thank the laboratory of Prof. Wu Yuxiang for the use of their equipment

Reference

[1] W. Gu, W. Zhang, M. Kavehrad, “Three-dimensional light positioning algorithm with filtering techniques for indoor environments [J],” *Opt. Eng.*, vol. 53, no. 10, pp. 107107–107107, 2014.
[2] J. Fang, Z. Yang, S. Long “High-speed indoor navigation system based on visible light and mobile phone [J],” *IEEE Photon. J.*, vol. 9, no. 2, Apr. 2017, Art. no. 8200711.
[3] T. H. Do and M. Yoo, “An in-depth survey of visible light communication based positioning systems [J],” *Sensors*, vol. 16, no. 5, 2016, Art. no. E678.
[4] W. Zhang and M. -A. Kavehrad, “2-D indoor localization system based on visible light,” in *Proc. IEEE Photon. Soc. Summer Topical Meet. Series*, 2012, pp. 80–81.
[5] W. Guan *et al.*, “High precision three-dimensional iterative indoor localization algorithm using code division multiple access modulation based on visible light communication [J],” *Opt. Eng.*, vol. 55, no. 10, Oct. 1, 2016, Art. no. 106105.

[6] W. Guan, Y. Wu, S. Wen, Y. Chen, and H. Chen, "Indoor positioning technology of visible light communication based on CDMA modulation [J]," *Acta Optica Sinica*, vol. 36, no. 11, pp. 66–74, Nov. 10, 2016.
[7] W. Guan *et al.*, "A novel three-dimensional indoor positioning algorithm design based on visible light communication [J]," *Opt. Commun.*, vol. 392, pp. 282–293, Jun. 1, 2017.
[8] Q.-L. Li, J.-Y. Wang, H. Ting, and W. Yongjin, "Three-dimensional indoor visible light positioning system with a single transmitter and a singletilted receiver [J]," *Opt. Eng.*, vol. 55, no. 10, Oct. 1, 2016, Art. no. 106103.
[9] S.-H. Yang, H.-S. Kim, Y.-H. Son, and S.-K. Han, "Three-dimensional visible light indoor localization using AOA and RSS with multiple optical receivers [J]," *J. Lightwave Technol.*, vol. 32, no. 14, pp. 2480–2485, Jul. 15, 2014.
[10] W. Gu, M. Kavehrad, and M. Aminikashani, "Three-dimensional indoor light positioning algorithm based on nonlinear estimation [C]," in *Proc. SPIE OPTO*, 2016, vol. 97720V.
[11] L. Yin, X. Wu, and H. Haas, "Indoor visible light positioning with angle diversity transmitter [C]," in *Proc. IEEE Veh. Technol. Conf.*, Jan. 25, 2015, pp. 1–5.
[12] Y. Wang, Y. Gong, and Z. Shi, "Research on the collinear equation model of visual positioning based on visible light communication [J]," *MATEC Web Conf.*, vol. 22, Jul. 9, 2015, Art. no. 02003.
[13] Y. Xu, J. Zhao, J. Shi, and N. Chi, "Reversed three-dimensional visible light indoor positioning utilizing annular receivers with multi-photodiodes [J]," *Sensors (Switzerland)*, vol. 16, no. 8, Aug. 8, 2016, Art. no. E1254.
[14] P. J. M. Van Laarhoven and E. H. L. Aarts, *Simulated Annealing: Theory and Applications*. Berlin, Germany:Springer, 1988.
[15] W. Guan, Y. Wu, C. Xie, H. Chen, Y. Cai, and Y. Chen, "High-precision approach to localization scheme of visible light communication based on artificial neural networks and modified genetic algorithms," *Opt. Eng.* vol. 56, no. 10, 2017, Art. no. 106103, doi: 10.1117/1.OE.56.10.106103.
[16] N. Li, J. Chen, Y. Yuan, X. Tian, Y. Han, and M. Xia, "A Wi-Fi Indoor Localization Strategy Using Particle Swarm Optimization Based Artificial Neural Networks [J]," *Int. J. Distrib. Sensor Netw.*, vol. 2016, 2016, Art. no. 33.
[17] D. S. Lee, Y. W. Seo, and K. C. Lee, "An adjusted simulated annealing approach to particle swarm optimization," *Asian Conf. Intell. Inf. Database Syst.*, vol. 6592, pp. 566–575, 2011.
[18] D. Ganti, W. Zhang, and M. Kavehrad, "VLC-based indoor positioning system with tracking capability using Kalman and particle filters," in *Proc. IEEE Int. Conf. Consum. Electron.*, 2014, pp. 476–477.
[19] Nan Wu, Lihui Feng, and Aiying Yang, "Localization accuracy improvement of a visible light positioning system based on the linear illumination of LED sources," *IEEE Photon. Soc.*, vol. 9, no. 5, Oct. 2017, Art. no. 7905611.
[20] Y. Hou, S. Xiao, M. Bi, Y. Xue, W. Pan, and W. Hu, "Single LED beacon-based 3-D indoor positioning using off-the-shelf devices [J]," *IEEE Photon. J.*, vol. 8, no. 6, Dec. 2016, Art. no. 6806211.
[21] W.-P. Guan, S.-S. Wen, H.-X. Hu, and Y.-C. Chen, "Research on visible light communication system based on hybrid modulation technique [J]," *J. Optoelectron. Laser*, vol. 26, no. 11, pp. 2125–2132, Nov. 15, 2015.
[22] G. Weipeng *et al.*, , "Research on visible light communication receiving system based on artificial neural networks [J]," *Chin. J. Lasers*, vol. 42, no. 11, p. 1105002, Nov. 10, 2015.
[23] T. Komine and M. Nakagawa, "Fundamental analysis for visible-light communication system using LED lights [J]," *IEEE Trans. Consum. Electron.*, vol. 50, no. 1, pp. 100–107, Feb. 2004.
[24] S.-H. Yang, E.-M. Jeong, D.-R. Kim, H.-S. Kim, Y.-H. Son, and S.-K. Han, "Three-dimensional localization based on visible light optical wireless communication," in *Proc. Int. Conf. Ubiquitous Future Netw., ICUFN*, pp. 468–469, 2013, pp. 468–469.